TU Delft

Delft University of Technology

Document Version
Final published version

Licence
Dutch Copyright Act (Article 25fa)

Citation (APA)
Cremer, J. L. (2026). Assessing Maintenance of Medium Voltage Cable Networks Under Time-Varying Loading. *IEEE Transactions on Power Delivery*, *41*(5), 2128-2140. https://doi.org/10.1109/TPWRD.2026.3681694

Important note
To cite this publication, please use the final published version (if applicable).
Please check the document version above.

Copyright
In case the licence states “Dutch Copyright Act (Article 25fa)”, this publication was made available Green Open Access via the TU Delft Institutional Repository pursuant to Dutch Copyright Act (Article 25fa, the Taverne amendment). This provision does not affect copyright ownership.
Unless copyright is transferred by contract or statute, it remains with the copyright holder.

Sharing and reuse
Other than for strictly personal use, it is not permitted to download, forward or distribute the text or part of it, without the consent of the author(s) and/or copyright holder(s), unless the work is under an open content license such as Creative Commons.

Takedown policy
Please contact us and provide details if you believe this document breaches copyrights.
We will remove access to the work immediately and investigate your claim.

This work is downloaded from Delft University of Technology.

Assessing Maintenance of Medium Voltage Cable Networks Under Time-Varying Loading

Jochen Lorenz Cremer, *Senior Member, IEEE*

***Abstract*—The electrification and ongoing energy transition lead to systematic changes in electricity loading and variability in power systems. Distribution systems were designed for regular operating patterns, assuming constant low loading. Now, operators need to assess whether their assets can withstand more, as well as time-varying loading. Operating the system at or near its ampacity potentially accelerates thermal ageing, so the question arises: 'how much can one operate at the limits while keeping maintenance and failures low?' This paper introduces a novel approach that derives a time-varying Weibull approximation of failure rates using thermal models and provides a shortcut method to quantify maintenance implications under time-varying loading for heterogeneous MV cable populations. The case studies investigate a dataset from Denmark and the Oberrhein Medium Voltage (MV) system in Germany, studying ageing assets and the interplay with loading, and replacement paradigms of two different cable insulation types. The studies demonstrate that a small fraction of 25% of old, low-quality cables leads to 82% of failures, and 1.4% of the time of highest loading can cause 46% of cable ageing. The case studies also demonstrate that maintenance needs may be between $10-300$ times higher under future loading conditions associated with the energy transition, specifically in networks that have older PILC cables. This paper provides a new tool for operators to plan maintenance under more realistic, future operating conditions.**

***Index Terms*—Failure analysis, network reliability, power distribution maintenance, power distribution reliability, power system reliability, Weibull distributions.**

I. Introduction

A STRATEGY to decarbonise our economy is the electrification of the private and industrial sectors. Electrification requires operating the distribution and transmission systems more smartly. Smarter tooling ultimately enables Distribution System Operators (DSOs) to operate existing assets at higher capacity, possibly surpassing specified power ratings for short periods. These operating ratings typically ensure the reliability of these assets, providing an expectation of their lifespan [1]. DSOs use these estimations of lifespan in their maintenance plans. However, electrification and renewable integration associated with the energy transition alter electricity operating conditions and increase system loading. The actual loadings may surpass even the rated loading, reducing the lifespan of the overloaded assets [2]. The lifespans may currently be overestimated at scale.

Overestimating the lifespan potentially leads to a large maintenance burden in the future, and in the worst case drastic increase in failures of power network assets, as it can already be experienced in other sectors, like railway and road transportation. The loading of the German railway system increased, and an aged infrastructure (among other reasons) led to more frequent technical failures due to asset fatigue (e.g. [3]). Roads designed decades ago experience types of vehicles (e.g. SUVs) that are heavier than vehicles assumed at the road network's design. Heavier vehicles lead to fast degradation of pavements (degradation $\propto$ (vehicle weight)^4 [4]) and to more frequent required maintenance of pavements, as one can observe in many countries.

Past research statistically analysed the reliability of MV cables, and experiments investigated the impact of loading on ageing. Cable failures account for a major share of MV network faults [5] and are typically analysed as a function of service time to support maintenance planning [6]. Failure rates increase with service time as for most physical assets, such as cables. However, most failure models assume loading does not change over time, i.e., no systematic increase or decrease over years. MV networks commonly include XLPE and PILC cables, where ageing PILC assets, often exceeding 50 years of service, contribute disproportionately to failure rates and reinvestment needs. In MV networks, the need for reinvestment to replace these old cables is well recognised [5], and a drastic increase in age-related failure rates in PILC cables can currently be observed in Denmark [7], [8], [9]. Increasing the loading across the network in the upcoming years through electrification may reduce the lifespan and increase failure rates at scale. The realisation of distributed energy resources (DERs) increases the peaks of loadings [2], which specifically reduces cable lifetime. This research aims to estimate failure rates under varying loading conditions over time in a distribution of aged cables.

Planning for the maintenance of MV cables [10] often involves either applying monitoring to the cables or assuming static loading conditions, which does not require monitoring devices. Parameters that impact ageing and failure rates are load estimates [11] and average temperature [12], among others. The temperature increases with time when the loading increases. Prolonged high cable temperatures lead to faster degradation ('overheating'). Currently, performing preventive maintenance requires the early identification and localization of overheated

Received 6 October 2025; revised 5 February 2026; accepted 4 April 2026. Date of publication 7 April 2026; date of current version 25 September 2026. This work was supported in part by Dutch Research Council, Veni Talent Program under Grant #19161, and in part by Delft AI Initiative Program. Paper no. TPWRD-01358-2025.

The author is with the Department of Electrical Sustainable Energy, Delft University of Technology, 2628 CD Delft, The Netherlands, and also with the Centre for Energy, Austrian Institute of Technology, 1210 Vienna, Austria (e-mail: j.l.cremer@tudelft.nl).

Digital Object Identifier 10.1109/TPWRD.2026.3681694

1937-4208 © 2026 IEEE. All rights reserved, including rights for text and data mining, and training of artificial intelligence and similar technologies. Personal use is permitted, but republication/redistribution requires IEEE permission. See https://www.ieee.org/publications/rights/index.html for more information.

Authorized licensed use limited to: TU Delft Library. Downloaded on October 08,2026 at 07:45:28 UTC from IEEE Xplore. Restrictions apply.

sections using power line communication, applying local measurement devices [13], [14]. If overheated sections are repeatedly identified, the operator acts to replace the specific line or implement other mitigation actions. Recent work also explores data-driven condition monitoring frameworks using machine learning to estimate cable health indices from multi-source inspection and operational data, enabling predictive and automated asset management strategies [15]. The smart cable guard system [16] can monitor the condition of a cable, enabling root cause analysis to prevent failures. The temperatures of cables can be accurately estimated, given the loading [17]; however, these systems can not estimate the lifespan of a single cable or the population of cables, which remains a challenging task. Through experiments, [18] assesses the relationship between ageing and loading above rated temperature, showing that short-term emergency loading and frequent overloads lead to a thermal memory effect. This effect leads to higher failure rates. For example, [18] states that raising the rated operating temperature from 90 °C to $95-105$ °C significantly reduces the lifespans of XLPE cables from $40-60$ to $7-30$ years. However, experiments show exposing old 110kV XLPE cables at the ampacity 900A leads to exceeding temperatures 90 °C after 5h-8h [19]. For PILC cables, [20] shows a clear dependency of the p-factor on the cable age and history, where cables of ages $0-60$ were tested [21]. The Montsinger approach [22] and Arrhenius approach can estimate the lifetime as a function of the stressor (temperature) [2]. The accelerated failure time model assumes accelerated or decelerated ageing relative to a reference, and can predict lifetime and failure rates for varying operating conditions [23]. Additionally, probabilistic prognostic approaches based on dynamic state transition models and Bayesian filtering have been proposed to predict insulation degradation trajectories and remaining useful life under varying loading and environmental conditions [24]. Frequently, for reliability studies, the failure rate is modelled with a Weibull distribution, providing statistical tools to estimate lifetimes and failure rates. The Common Network Asset Indices Methodology (CNAIM) estimates lifespan based on individual asset data [25]. These estimations of the lifespan and failure rates for a population of cables with varying ages were possible in the past, as the loading levels remained fairly constant over the years. However, currently, the failure rate is not considered to change with time as the loading patterns change at scale, possibly sometimes exceeding rated temperatures and accelerating ageing. Not estimating the lifespan and failure rate, considering projections of future loading conditions in the electrification can potentially lead to high risks for society, underestimating costs for maintenance and cable replacements.

Existing reliability models typically assume stationary loading conditions and therefore do not explicitly capture systematic transitions in loading distributions occurring during the energy transition. Consequently, current approaches cannot fully represent the interaction between thermally driven ageing processes and long-term structural changes in operating conditions. This paper introduces a general approach linking thermal ageing physics with non-stationary reliability theory, allowing analytical estimation of population-level failure evolution under load transition scenarios. More specifically, this paper develops methods to help assess the risk of overestimating expected lifespan and maintenance under loading changes associated with the energy transition. This paper focuses on a systematic change in the distribution of loading levels toward higher loading levels. Specifically, this paper contributes by

1) method to estimate effective ageing for a distribution of cables with varying age and loading exposure over time
2) shortcut method to assess maintenance increase at the limits of systemic loading changes for a population of cables. The method is developed for *Run-to-failure*, *Replace-all*, and *Preventive* maintenance strategies.

Case studies focus on power systems with PILC and XLPE MV cables. The studies apply asset data from Danish distribution grids and the Oberrhein MV system in Germany. The studies investigate the impact of thermal ageing on failure rates by applying the Arrhenius and Montsinger models. Then, the studies investigate the impact of time-varying loading associated with energy-transition scenarios on a network with diverse cable ages. Studies then focus on the proposed shortcut method to assess three maintenance approaches, comparing the states before and after the energy transition.

This paper is structured as follows. Section II investigates the reliability of MV cables, developing the methodology for ageing under time-varying loading. Section III develops the shortcut methods to investigate the three maintenance strategies. Section IV is the case study, and Section V concludes.

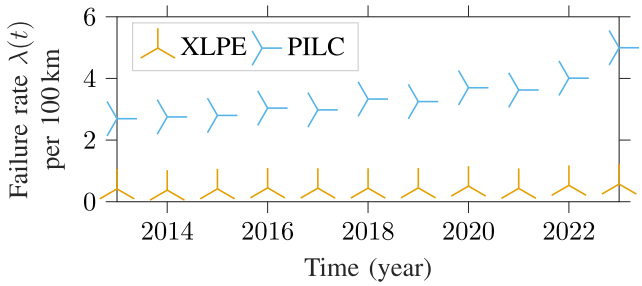


Fig. 1. Failures of medium voltage cables in Denmark. The increase is due to age-related failure (applied from [7], [8], [9]).

II. Reliability of MV Cables

A recent statistic in Fig. 1 shows a drastic increase in age-related failure rates over the last four years in PILC cables [7], [8]. These statistics are typically analysed as a function of service time and often do not account for the exposure of cables to different loading levels. However, cables located in parts of the network experiencing higher loading may fail earlier than those operated at lower loading levels. As shown in [2], even if the average utilisation does not increase or increases only slightly, the expansion of DERs can lead to short periods of high cable utilisation (see Fig. 2), which can significantly reduce cable lifetimes.

We consider a medium voltage network that has a set of cables Ω^C that are considered with a unit length. $\rho_A(a)$ is the probability density function of cable service times ('age' a). We

Authorized licensed use limited to: TU Delft Library. Downloaded on October 08,2026 at 07:45:28 UTC from IEEE Xplore. Restrictions apply.

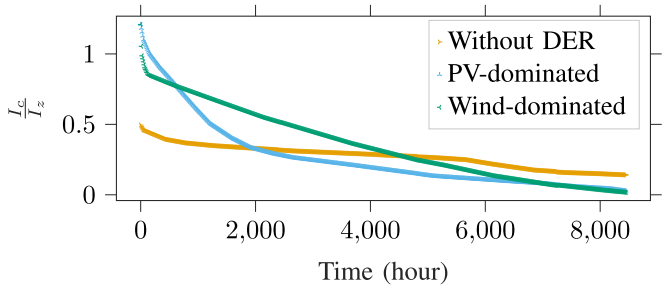


Fig. 2. The annual cable utilisation for three energy scenarios (applied from Fig. 10 in [2]).

consider ageing-related failures with the Weibull rate

$$\lambda(a) = \frac{\beta}{\hat{\eta}_r}\left(\frac{a}{\hat{\eta}_r}\right)^{\beta-1} \tag{1}$$

where $\beta > 1$ and the characteristic lifetime $\hat{\eta}_r > 1$. At $a = \hat{\eta}_r$, 63.2% of assets failed. The expected failures per year are

$$F = |\Omega^C| \int_0^\infty \lambda(a)\, \rho_A(a)\, da \tag{2}$$

where $|\Omega^C|$ is the cardinality of the set Ω^C.

Operational conditions impact the service life of medium voltage cables, specifically when exceeding ampacities. As Fig. 2 shows, ampacities may more frequently be exceeded in grids with DERs than without DERs [2]. However, most maintenance approaches assume constant operation $\left(\frac{d\lambda(a)}{dt} = 0\right)$ from when the grid was designed without DERs. However, this assumption no longer holds. Failing to consider changes in operational maintenance planning may increase failure rates and lead to higher maintenance needs. In response, this paper aims to estimate the number of cable replacements $N(t)$ required to maintain service reliability ($\frac{dF}{dt} = 0$) under evolving loading conditions. The grid undergoes the transition from t_0 (without DER) to t_1 (with wind and PV DERs). We introduce the distribution of loading $\rho_T(t)$ that changes with time t, and derive the Weibull failure rate $\lambda(a,t)$ for an age distribution $\rho_A(a)$ of cables. As we demonstrate, this extension can be used to estimate

- the maintenance increase $\frac{N(t_1)}{N(t_0)}$ to keep reliability constant $\left(\frac{dF}{dt} = 0\right)$
- the failure rate increase $\frac{F(t_1)}{F(t_0)}$ if the maintenance efforts are not adjusted $N(t_1) = N(t_0)$

A. Thermal Ageing of MV Cables

We exemplarily focus on failures caused by thermal ageing, which is the main ageing mechanism for PILC cables, and thermal ageing increases as the load increases. Nonetheless, studies show that failures of cable joints cause 45 % MV cable failures [2], [26]. These are not investigated in this work. We consider the insulation material as the cause of failure. The conductor temperature T can be estimated with

$$T(\tau) = T_a + (T_{max} - T_a) \cdot \left(\frac{|I_c(\tau)|}{I_z}\right)^2 \tag{3}$$

that is a function of the conductor current $I_c(\tau)$ at time τ, maximal temperature T_{max}, and the rated current I_z for the ambient temperature T_a [27]. (3) does not consider that the temperature depends on the electrical resistance. Neglecting temperature-dependent electrical resistance introduces a modelling approximation whose impact increases with loading levels. However, for moderate loading ranges typically below ampacity, the approximation provides a tractable analytical representation of temperature dynamics and remains widely applied in thermal rating studies. The sensitivity of this approximation is evaluated in Section IV-B and compared with the extended formulation (49) provided in the Appendix. The conductor temperature can also be estimated using real-time temperature rating [17]. The Arrhenius model estimates the thermal ageing acceleration factor as

$$r(T) = \frac{\eta_r}{\eta} = \exp B\left(\frac{1}{T_r} - \frac{1}{T}\right) \tag{4}$$

where the mean lifetime η_r and $B > 0$ is assumed to be experimentally recorded at the reference temperature T_r. The Arrhenius model can be applied to the insulation material in XLPE cables. Montsinger's approach can be applied to estimate the lifetime of insulation material in PILC cables [22]. The Montsinger ageing acceleration factor

$$r(T) = \frac{\eta_r}{\eta} = 2^{\frac{T-T_r}{\Delta T}} \tag{5}$$

is doubled for increasing increments $\Delta T > 0$ of temperature T [27]. The Montsinger model is an empirical approximation derived from accelerated ageing experiments and is primarily valid when thermal degradation is the dominant ageing mechanism. Its applicability may be limited in field conditions where additional factors such as moisture ingress, mechanical stress, or installation defects significantly influence insulation ageing. In this work, the model is applied to represent thermally driven ageing at the system level. The effective age $A(a,t)$ for a cable that is $a(t) = t - t_0$ years in service at time t is

$$A(a,t) = \int_{t-a}^{t} r(T(\tau))d\tau \tag{6}$$

considering the temperature trajectory $T(t)$. t_0 is the installation time of a cable.

The cumulative Weibull hazard with effective age u is

$$H(u) = \left(\frac{u}{\hat{\eta}_r}\right)^{\beta} \tag{7}$$

with the characteristic age $\hat{\eta}_r = \frac{\eta_r}{\Gamma\left(1+\frac{1}{\beta}\right)}$, i.e. η_r is the mean life and $\hat{\eta}_r$ is for the Weibull scale.

We can derive the failure rate as the change of hazard in time, i.e.

$$\lambda(a,t) = \frac{d}{dt}H(A(a,t)) = \left(\frac{\beta}{\hat{\eta}_r}\right)\left(\frac{A(a,t)}{\hat{\eta}_r}\right)^{\beta-1} r(T(t)) \tag{8}$$

where $u = A(a,t)$. The formulation in (8) provides a conceptual extension of classical Weibull reliability modelling by embedding time-dependent stress histories into the hazard formulation

Authorized licensed use limited to: TU Delft Library. Downloaded on October 08,2026 at 07:45:28 UTC from IEEE Xplore. Restrictions apply.

through the effective age functional $A(a,t)$. Unlike conventional approaches that consider ageing solely as a function of service time, this approach enables reliability modelling under temporally evolving stress environments while preserving analytical tractability. This formulation therefore establishes a direct connection between physics-of-failure ageing models and population-level survival analysis under non-stationary operating conditions.

B. Constant Loading

When assuming a constant loading $I_c(t) = I_c$ and temperature $T(t) = T$, the effective age is $A(a,t) = a\frac{\eta_r}{\eta(T)}$, and the failure rate of the Arrhenius-Weibull model simplifies to

$$\lambda(a,T) = \frac{\beta}{\hat{\eta}(T)}\left(\frac{a}{\hat{\eta}(T)}\right)^{\beta-1} \tag{9}$$

The characteristic lifespan $\hat{\eta}(T)$ can be estimated at a constant temperature T as

$$\hat{\eta}(T) = \frac{\hat{\eta}_r}{r(T)} \tag{10}$$

and applying (4) or (5) for XLPE or PILC, respectively.

C. Time-Varying Loading Distribution

Analogue to the Miner's cumulative damage model [28], [29], we consider that different stress levels weighted by their cycle times lead to failure. This formulation assumes cumulative damage accumulation and does not explicitly model potential thermal recovery or relaxation effects during periods of reduced loading. This assumption is consistent with commonly applied accelerated ageing and Miner-type damage accumulation approaches in insulation reliability modelling, where degradation is primarily driven by peak thermal exposure. As the cumulation, not the sequence, matters, one can also take an estimate of the probability density function of loading conditions $\rho_T(T,t)$ at time t, and define the effective ageing acceleration as

$$\overline{r}(t) = \int_{-\infty}^{\infty} r(T)\,\rho_T(T,t)\,dT \tag{11}$$

and the effective age

$$\overline{A}(a,t) = \int_{t-a}^{t} \overline{r}(s)ds \tag{12}$$

Then the cumulative hazard is

$$H(a,t) = \left(\frac{\overline{A}(a,t)}{\hat{\eta}_r}\right)^{\beta} \tag{13}$$

and the failure rate

$$\lambda(a,t) = \frac{\beta}{\hat{\eta}_r}\left(\frac{\overline{A}(a,t)}{\hat{\eta}_r}\right)^{\beta-1}\overline{r}(t) \tag{14}$$

D. Steady-State Seasonality

When each year has a similar load distribution $\rho(T)$, we can assume a steady-state of the load distribution loading $\rho_T(T,\tau) = \rho(T)$ that is constant in time τ from year to year. Then, one can assume a constant acceleration factor $\overline{r}(\tau) = \overline{r}$ with

$$\overline{r} = \int_{-\infty}^{\infty} r(T)\,\rho_T(T)\,dT \tag{15}$$

and the characteristic lifetime

$$\hat{\eta} = \frac{\hat{\eta}_r}{\overline{r}} \tag{16}$$

E. Dynamics of Seasonal Load

However, the energy transition changes the loading distribution from year to year, and the above does not hold any longer. We can assume piecewise changes of the distribution of loadings $\rho_k(T)$ from season k to season $k+1$ during the transition from low-DER to high-DER loading conditions. We assume the duration of a season as $\Delta\tau_k = \tau_{k+1} - \tau_k$ and the time interval is $[\tau_k, \tau_{k+1})$. Then, the temperature distribution is

$$\rho_T(T,t) = \rho_k(T), \quad \text{if} t \in [\tau_k, \tau_{k+1}) \tag{17}$$

and we use (11) in season k as the expected ageing acceleration

$$\overline{r}_k = \int_{-\infty}^{\infty} r(T)\,\rho_k(T)\,dT \tag{18}$$

We can then obtain the effective age

$$\overline{A}(a,t) = \sum_{k\in\kappa(a,t)} \Delta\tau_k\,\overline{r}_k, \tag{19}$$

for a cable age a at time t that has been in service during the seasons $\kappa(a,t) = \{k : t-a \le \tau_k \le \tau_{k+1} \le t\}$. Using $\overline{r}_k$ and $\overline{A}(a,t)$ in (14) gives the failure rate $\lambda(a,t)$.

F. Time-Varying Loading in the Transition to Higher DERs

One can model the transition between loading regimes using a logistic function

$$\rho_T(T,\,t) = \rho_0(T) + \frac{\Delta\rho_T(T)}{1+\exp\{-c_1(t-c_2)\}} \tag{20}$$

where $\Delta\rho_T = \rho_1(T) - \rho_0(T)$. $c_1 > 0$ and c_2 are stylised descriptors of transition dynamics rather than calibrated physical parameters, where c_1 controls the speed of loading changes associated with DER integration and c_2 represents the characteristic midpoint of a typically multi-decade transition period. We then take $\rho_T(T,\,t)$ in (11) and (12) and change the order of integration to

$$\overline{A}(a,t) = \int_{-\infty}^{\infty} r(T)\int_{t-a}^{t}\rho_T(T,s)\,ds\,dT \tag{21}$$

We consider the inner integral

$$\begin{aligned}\int_{t-a}^{t}\rho_T(T,s)\,ds &= \int_{t-a}^{t}\rho_0(T) + \frac{\Delta\rho_T(T)}{1+e^{-c_1(s-c_2)}}\,ds \\ &= a\,\rho_0(T) + \frac{\Delta\rho_T(T)}{c_1}\ln\left(\frac{1+e^{c_1(t-c_2)}}{1+e^{c_1(t-a-c_2)}}\right)\end{aligned} \tag{22}$$

Authorized licensed use limited to: TU Delft Library. Downloaded on October 08,2026 at 07:45:28 UTC from IEEE Xplore. Restrictions apply.

We can now write the effective age over the time window of a cable with age a as

$$\overline{A}(a,t) = a\int_{-\infty}^{\infty} r(T)\,\rho_0(T)\,dT + \frac{1}{c_1}\ln\left(\frac{1+e^{c_1(t-c_2)}}{1+e^{c_1(t-a-c_2)}}\right)\int_{-\infty}^{\infty} r(T)\Delta\rho_T(T)\,dT \tag{23}$$

We define the limits of the effective age

$$\overline{A}_0(a) := \lim_{t\to-\infty}\overline{A}(a,t) = a\int_{-\infty}^{\infty} r(T)\,\rho_0(T)\,dT \tag{24}$$

$$\overline{A}_1(a) := \lim_{t\to+\infty}\overline{A}(a,t) = a\int_{-\infty}^{\infty} r(T)\,\rho_1(T)\,dT \tag{25}$$

before and after the energy transition, respectively. A compact way for the effective age is

$$\overline{A}(a,t) = \overline{A}_0(a) + \frac{1}{c_1 a}\ln\left(\frac{1+e^{c_1(t-c_2)}}{1+e^{c_1(t-a-c_2)}}\right)\left(\overline{A}_1(a) - \overline{A}_0(a)\right) \tag{26}$$

that in (14) can compute the failure rate in time $\lambda(a,t)$.

III. Maintenance Strategies

DSOs can apply different maintenance and replacement strategies for their assets [30], for example:

1) Run-to-Failure: This strategy replaces cables after failure. The expected number of cables annually replaced is

$$N(t) = |\Omega^C|\int_0^{\infty}\lambda(a,t)\,\rho_A(a,t)\,da \tag{27}$$

where $\rho_A(a,t)$ is the age distribution of the cables that may change with time t. $|\Omega^C|$ is the number of cables in the network. *Run-to-failure* could be a viable strategy in a grid that runs at very low loading conditions, as some cables operated in low, ideal conditions can last up to 200 years.

2) Replace-All: This strategy regularly replaces cables when their failure rate is above a specified threshold λ_R, or applies a replacement time a_R that can be converted by $\lambda_R(t) = \lambda(a_R(t),t)$ in (8). At constant loading, one can apply

$$a_R = \hat{\eta}\left(\lambda_R\frac{\hat{\eta}}{\beta}\right)^{\frac{1}{\beta-1}} \tag{28}$$

from (9). The number of cables annually replaced can be estimated as

$$N(t) = |\Omega^C|\left(\int_0^{a_R}\lambda(a,t)\,\rho_A(a,t)\,da + \int_{a_R}^{\infty}\rho_A(a,t)\,da\right) \tag{29}$$

considering the replacement in response to a failure, and the share of cables that surpassed the replacement time a_R. This is typically an expensive strategy. A typical replacement time for PILC is around $a_R = 50$ years [2].

3) Preventive Maintenance: Applying preventive maintenance reduces failures [31]. The strategy regularly assesses the remaining useful life or health index for each cable $c \in \Omega^C$. Subsequently, the cables are assigned to 'keep' $\Omega^K \leftarrow \Omega^K \cup \{c\}$, to perform 'preventive maintenance' $\Omega^M \leftarrow \Omega^M \cup \{c\}$ or to 'replace' $\Omega^R \leftarrow \Omega^R \cup \{c\}$ [32]. The assignment of cables in these three categories $\Omega^C = \Omega^K \cup \Omega^M \cup \Omega^R$ can be economically optimised [33]. Depending on the level of maintenance, one can expect a reduction in the failure rate

$$\lambda_c(a,t) = \lambda(a,t)\,(1-x_c), \tag{30}$$

where $x_c \geq 0$ corresponds to the maintenance carried out on cables $c \in \Omega^M$, e.g. $x_c = 0$ if no maintenance was carried out. The distribution of maintenance levels carried out for cables at age a is $\rho_{XA}(x,a)$ that is assumed steady in time. The number of cables that are annually expected to fail is

$$F(t) = |\Omega^C|\int_0^{\infty}\lambda(a,t) \times\left(\int_0^{\infty}(1-x)\rho_{XA}(x,a)\,dx\right)\rho_A(a,t)\,da \tag{31}$$

The expected number of cables annually to maintain is $|\Omega^M|$, and the cables to replace is

$$N(t) = F(t) + |\Omega^R| \tag{32}$$

B. Assessing Maintenance Strategies With Shortcuts

The maintenance strategies *Replace-all*, *Run-to-failure*, and *Preventive Maintenance* can be analysed for time-varying load with (27), (29) and (31), respectively. We start considering a loading profile that is steady-state in seasonality (Section II-D) and does not change over years, i.e. $\overline{r}_k = \overline{r}_{k+1} = \overline{r}\ \ \forall k$, then (15) simplifies to the constant acceleration factor

$$\overline{r}(t) = \overline{r} \tag{33}$$

that can be computed with (15). The characteristic lifetime $\hat{\eta}$ can be computed by (16). The effective age is

$$\overline{A}(a) = a\,\overline{r} \tag{34}$$

and applying (14) leads to the failure rate

$$\lambda(a) = \frac{\beta\,\overline{r}}{\hat{\eta}_r}\left(\frac{\overline{A}(a)}{\hat{\eta}_r}\right)^{\beta-1} = \frac{\beta}{\hat{\eta}}\left(\frac{a}{\hat{\eta}}\right)^{\beta-1} \tag{35}$$

Then, we consider the limits before and after the energy transition ((24) and (25)): $\hat{\eta}_0$ and $\overline{r}_0$ considers the load distribution $\rho_0(T)$ at time t_0 and $\hat{\eta}_1$ and $\overline{r}_1$ consider the load distribution $\rho_1(T)$ at time t_1, respectively.

1) Run-to-Failure: To assess the increase in maintenance $\frac{N(t_1)}{N(t_0)}$ in (27), assuming the cable network size $|\Omega^C|$ is constant and the age distribution ρ_A also stays constant

$$\frac{N(t_1)}{N(t_0)} = \frac{\int_0^{\infty}\frac{\beta}{\hat{\eta}_1}\left(\frac{a}{\hat{\eta}_1}\right)^{\beta-1}\rho_A(a)\,da}{\int_0^{\infty}\frac{\beta}{\hat{\eta}_0}\left(\frac{a}{\hat{\eta}_0}\right)^{\beta-1}\rho_A(a)\,da} = \left(\frac{\hat{\eta}_0}{\hat{\eta}_1}\right)^{\beta} = \left(\frac{\overline{r}_1}{\overline{r}_0}\right)^{\beta} \tag{36}$$

Authorized licensed use limited to: TU Delft Library. Downloaded on October 08,2026 at 07:45:28 UTC from IEEE Xplore. Restrictions apply.

2) Replace-All: Assessing the increase in maintenance $\frac{N(t_1)}{N(t_0)}$ in (29) where we assume the same replacement age a_R leads to

$$\frac{N(t_1)}{N(t_0)} = \frac{\int_0^{a_R} \frac{\beta}{\hat{\eta}_1}\left(\frac{a}{\hat{\eta}_1}\right)^{\beta-1} \rho_A(a)\,da + \int_{a_R}^{\infty} \rho_A(a)\,da}{\int_0^{a_R} \frac{\beta}{\hat{\eta}_0}\left(\frac{a}{\hat{\eta}_0}\right)^{\beta-1} \rho_A(a)\,da + \int_{a_R}^{\infty} \rho_A(a)\,da} \tag{37}$$

We can simplify to

$$\frac{N(t_1)}{N(t_0)} = \frac{\beta\,(\hat{\eta}_1)^{-\beta} \int_0^{a_R} a^{\beta-1}\,\rho_A(a)\,da + \int_{a_R}^{\infty} \rho_A(a)\,da}{\beta\,(\hat{\eta}_0)^{-\beta} \int_0^{a_R} a^{\beta-1}\,\rho_A(a)\,da + \int_{a_R}^{\infty} \rho_A(a)\,da} \tag{38}$$

We introduce

$$\mu := \frac{\beta \int_0^{a_R} a^{\beta-1}\,\rho_A(a)\,da}{\int_{a_R}^{\infty} \rho_A(a)\,da} \tag{39}$$

and obtain

$$\frac{N(t_1)}{N(t_0)} = \frac{\hat{\eta}_1^{-\beta}\mu + 1}{\hat{\eta}_0^{-\beta}\mu + 1} = \frac{\overline{r}_1^{\beta}\mu + \hat{\eta}_r}{\overline{r}_0^{\beta}\mu + \hat{\eta}_r}. \tag{40}$$

$\frac{N(t_1)}{N(t_0)}$ may be further simplified if one has an analytic function of $\rho_A(a)$ or makes assumptions.

3) Preventive Maintenance: Assessing the increase in maintenance $\frac{N(t_1)}{N(t_0)}$ in the *Preventive Maintenance* strategy in (31) we assume the distribution of maintenance levels $\rho_{XA}(x,a)$ is constant

$$\kappa(a) := \int_0^{\infty} (1-x)\rho_{XA}(x,a)\,dx \tag{41}$$

The number of cables that are annually expected to fail in season t_0 is

$$F(t_0) = |\Omega^C| \int_0^{\infty} \frac{\beta}{\hat{\eta}_0}\left(\frac{a}{\hat{\eta}_0}\right)^{\beta-1} \kappa(a)\,\rho_A(a)\,da \tag{42}$$

and the change of failures is

$$\frac{F(t_1)}{F(t_0)} = \left(\frac{\hat{\eta}_0}{\hat{\eta}_1}\right)^{\beta} = \left(\frac{\overline{r}_1}{\overline{r}_0}\right)^{\beta} \tag{43}$$

Using (32) and assuming maintenance strategy is not changed ($\frac{|\Omega^R|}{dt} = 0$), an estimate of the cables requiring replacement is

$$N(t_1) = \left(\frac{\hat{\eta}_0}{\hat{\eta}_1}\right)^{\beta} F(t_0) + |\Omega^R| \tag{44}$$

or the maintenance increase is

$$\frac{N(t_1)}{N(t_0)} = \frac{\left(\frac{\hat{\eta}_0}{\hat{\eta}_1}\right)^{\beta} F(t_0) + |\Omega^R|}{F(t_0) + |\Omega^R|} \tag{45}$$

that can also be expressed in terms of $\overline{r}_1$ and $\overline{r}_0$.

C. Considering Individual Asset Data

We consider a DSO that applies the CNAIM or a similar collection of asset data. The DSO has access to the age a_c, maintenance x_c, and health index h_c of cables $c \in \Omega^C$. The cables $\Omega^C = \Omega^{CP} \cup \Omega^{CX}$ can be assigned to the two cable types Ω^{CP} PILC and Ω^{CX} XLPE cables, respectively. The DSO also operates a well-monitored MV system. The loading $T_c(t)$ is an actual recording or future estimates at time t and available for each cable c. We can compute $F(t)$ the expected number of failures during season t by converting (31) to a summation over all cables, then using (8) and (30) gives

$$\begin{aligned} F(t) &\approx \sum_{c\in\Omega^C} \lambda_c(a_c,t)\,\Delta t \\ &= \sum_{c\in\Omega^C} \left(\frac{\beta}{\hat{\eta}_r}\right)\left(\frac{A(a_c,t)}{\hat{\eta}_r}\right)^{\beta-1} r(T_c(t))\,(1-x_c)\,\Delta t \end{aligned} \tag{46}$$

where Δt is the length of a season t, and each cable has an individual effective age

$$A(a_c,t) = \int_{t-a_c}^{t} r(T_c(\tau))d\tau \tag{47}$$

from (6) considering the individual temperature trajectory $T_c(\tau)$ from the records and projections of loads over cable c. $r(T_c(\tau))$ follows (4) if $c \in \Omega^{CX}$ or (5) if $c \in \Omega^{CP}$, respectively. Also $\hat{\eta}_r$ and β differ for these two cable types. Assuming the time unit is in years, the number of annual replacements is then

$$N(t) = F(t) + |\Omega^R| \tag{48}$$

where $|\Omega^R|$ are the scheduled replacements during season t. The *Run-to-failure* maintenance strategy replaces only post-failure ($\Omega^R = \emptyset$) and does not apply preventive maintenance $x_c = 0\,\forall c$. The *Replace-all* strategy also does not apply preventive maintenance ($x_c = 0$) and replaces cables $\Omega^R \leftarrow \Omega^R \cup \{c\}$ if $a_c \geq a_R$. In the *Preventive Maintenance* strategy $\Omega^R \leftarrow \Omega^R \cup \{c\}$ if $h_c \leq h_R\,\forall c$ with the health index threshold for replacement h_R.

IV. Case Study

A. Study Settings, Test Networks and Data

The case study examines PILC and XLPE cables using two different thermal models, incorporating partly Danish cable data and thermal data from various sources. The study considers an initial cable population defined at time $t = 0$ based on Danish MV asset statistics, specifying the share, age distribution, and Weibull ageing parameters for PILC and XLPE cables. These cable populations are analysed using thermal ageing models and applied to the Oberrhein MV grid to evaluate failure behaviour under different loading scenarios derived from projected DER integration. The Oberrhein network is shown in Fig. 3 with the two cable types. For thermal ageing, the Arrhenius model (4) was applied to the XLPE cables, and the Montsinger approach (5) to the PILC cables. The cable data is reported in Table I. The Weibull parameter $\beta \approx 3$ was estimated for XLPE cables from Fig. 8 in [8], considering only cables older than 10 years. $\beta \approx 3.4$ was assumed for PILC cables from Fig. 7 in [5]. These shape parameters β need to be estimated separately for each cable population. The Danish data features PILC and XLPE cables, where $\Omega^C = \Omega^C_{\text{PILC}} \cup \Omega^C_{\text{XLPE}}$. We assume at $t = 0$ that the share of PILC cables in the network is $\frac{|\Omega^C_{\text{PILC}}|}{|\Omega^C|} = 0.25$ and the share of XLPE cables is $\frac{|\Omega^C_{\text{XLPE}}|}{|\Omega^C|} = 0.75$ as in the Danish MV

Authorized licensed use limited to: TU Delft Library. Downloaded on October 08,2026 at 07:45:28 UTC from IEEE Xplore. Restrictions apply.

TABLE I
PARAMETERS USED IN THERMAL AGING MODELS FOR XLPE ($1 \times 240\ \mathrm{mm}^2$) AND PILC ($3 \times 120\ \mathrm{mm}^2$) CABLES AT 12/20 KV

Parameter	Symbol	XLPE Cable	PILC Cable
Thermal aging model	–	Arrhenius	Montsinger
Aging slope / doubling factor	B, ΔT	16237 K	6.5°C
Reference lifetime	η_r	55 years	100 years
Reference conductor temperature	T_r	90°C	15°C
Maximum conductor temperature	$T_{\max}$	90°C	65°C
Ambient temperature (soil)	T_a	20°C	20°C
Temp. coefficient of resistance	α	4.03×10^{-3} 1/K (Al)	3.9×10^{-3} 1/K (Cu)
Rated current per conductor	I_r	313 A	302 A
Adjusted ampacity (standard conditions)	I_z	313 A	250 A

Notes: XLPE cable parameters are based on [34], [18], [35], [36]. PILC cable parameters are based on [2], [37]. Adjusted ampacities refer to standard buried installations at a 20°C soil temperature and a 1.0K·m/W thermal resistivity.

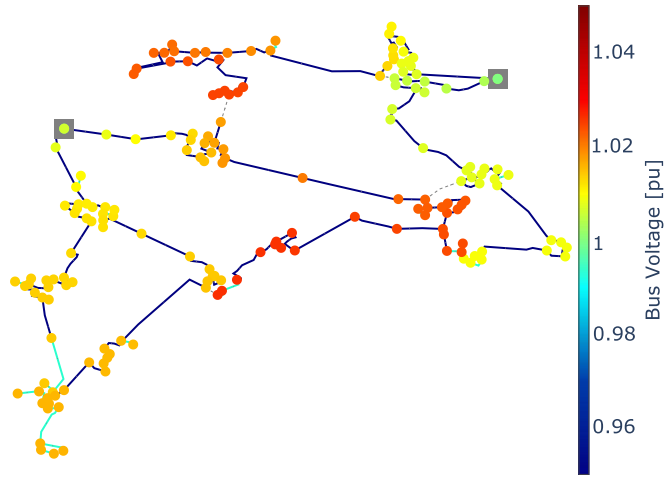


Fig. 3. Oberrhein MV network with PILC and XLPE cables.

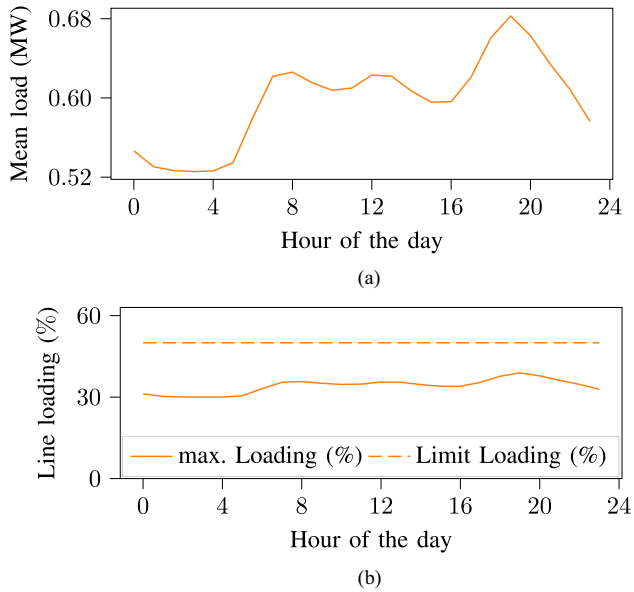


Fig. 4. Loading of the Oberrhein MV grid. (a) Mean load at buses over a 24-hour period. (b) Line loading (in %) relative to the maximum loading and limit loading.

grid in 2023 [8]. At the simulation time $t = 0$ years, the ages for PILC cables were assumed as a skewed normal distribution with $\mu = 58$, $\sigma = 21$ and $\delta = -3$. The ages for XLPE cables were assumed as a skewed normal distribution with $\mu = 10$, $\sigma = 15$ and $\delta = 3$. The cumulative distributions of these two skewed normal distributions roughly match Fig. 1 in [8]. Representative load scenarios for wind, PV, and without DERs are shown in Fig. 2, which was obtained from digitising Fig. 10 in [2].

[2] considers three DER scenarios in Germany until 2032 and used renewable projections from the Erneuerbare-Energien-Gesetz 2014. The MV system Oberrhein system applied spatial load distribution over a 24 h window. Fig. 4(a) shows the mean load across all buses. After solving the AC power flow, Fig. 4(b) shows the line loadings. The study assumes a maximal line loading of $I_z = 50\%$, and assumes lines have all the unit length. The 25% lines with the lowest average loading are assumed to be PILC and all other lines as XLPE cables (Fig. 3). The ages of the 181 lines were sampled from the initial skewed normal, age distributions at $t = 0$ (also shown later in Fig. 11). The *Replace-all* maintenance strategy assumes the replacement age $a_R = 50$ years. The *Preventive* strategy assumes $\frac{|\Omega^R|}{|\Omega^C|} = 0.002$ and $\kappa(a) = 0.98$ if $a \geq 25,\ 0$ otherwise. All simulations were implemented using Python 3.13.5 in Jupyter Notebook scripts with the NumPy 2.2.5 library. The MV Oberrhein grid model and AC power-flow calculations were performed using the Pandapower 3.1.2 package.

B. Thermal Ageing of MV Cables

This case study examines the thermal ageing of the insulation materials under different steady loading levels. To compute the conductor temperature T, (3) and (49) were applied, respectively, when neglecting or considering the temperature coefficient of resistance. To compute one data point (T, η_T) the current $I_c(\tau) = I_c$, ambient temperature T_a and temperature $T(\tau) = T$ were assumed in steady state, i.e. $\frac{dI(\tau)}{d\tau} = 0$, $\frac{dT_a(\tau)}{d\tau} = 0$ and $\frac{dT(\tau)}{d\tau} = 0$. (4) and (5) were used to compute lifespans η for PILC and XLPE, respectively. Fig. 5 confirms that the temperature increases with the loading, and the lifetime decreases. XLPE has a higher life expectancy than PILC cables. The lifetime drastically reduces when approaching the ampacity I_z in XLPE and approaching around 50% of I_z in PILC. A quantitative comparison between the simplified temperature model in (3) and the extended formulation in (49) shows that neglecting temperature-dependent resistance leads to limited deviations at moderate

Authorized licensed use limited to: TU Delft Library. Downloaded on October 08,2026 at 07:45:28 UTC from IEEE Xplore. Restrictions apply.

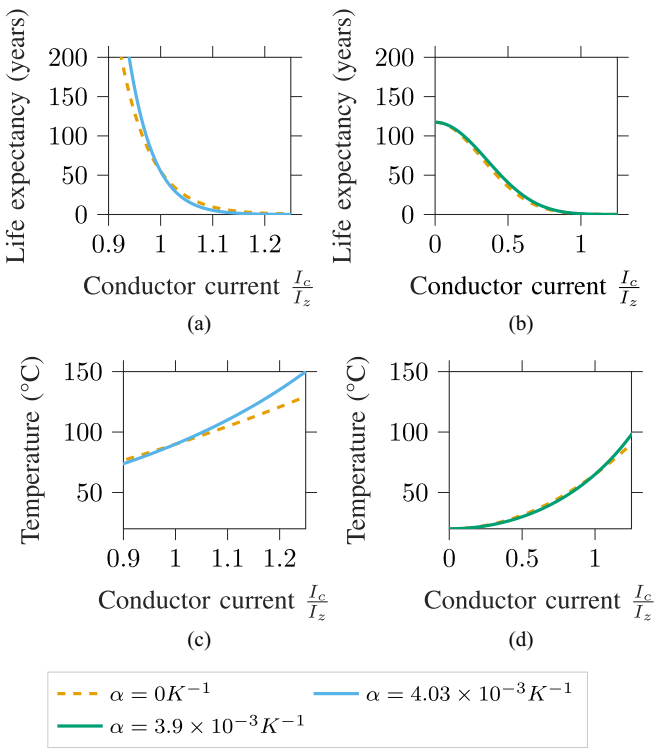


Fig. 5. Life expectancy and conductor temperature as functions of conductor current for XLPE and PILC cables. (a) Life expectancy of XLPE cables. (b) Life expectancy of PILC cables. (c) Conductor temperature of XLPE cables. (d) Conductor temperature of PILC cables.

loading levels but increasingly affects temperature and lifetime estimates close to ampacity. This study illustrates the fundamental behaviour of thermal ageing, demonstrating the importance of considering different loading levels in maintenance planning, as one cable at a lower loading level can last significantly longer than a cable at a higher loading level with respect to thermal ageing.

C. Time-Varying Loading

This study investigates effective ageing and failure rates under time-varying loading with two simulations: the first is explorative, applying basic loading profiles, and the second applies loading profiles during the energy transition. In the first explorative experiment, Fig 6(a) shows four different current profiles $I_c(t)$ in time, where one of them is constant $\frac{I_{c1}(t)}{I_z} = 0.5$. All four currents have the same average current over the 50 years. $\frac{I_{c2}(t)}{I_z}$ linearly increases in time, and $\frac{I_{c3}(t)}{I_z}$ is a step change at 25 years. $I_{c4}(t)$ applies the logistic function $\frac{I_{c4}(t)}{I_z} = 0.3 + \frac{0.4}{1+\exp\{-c_1(t-c_2)\}}$ with $c_1 = 0.2$ and $c_2 = 25$. Fig. 6(b) shows the instantaneous ageing acceleration factor $r(T(t))$ from (5) for a PILC cable. Fig. 6(c) exemplarily shows the effective age $A(10,t)$ for cables of actual age (service time) $a = 10$, i.e. (6) integrates $r(T(t))$ over a moving window of the previous 10 years. One can see that due to the integration of $r(T(t))$ that $A(10,t)$ drastically increases at the step change in I_{c3}. When comparing the linear increase I_{c4} with the step change I_{c3}, the

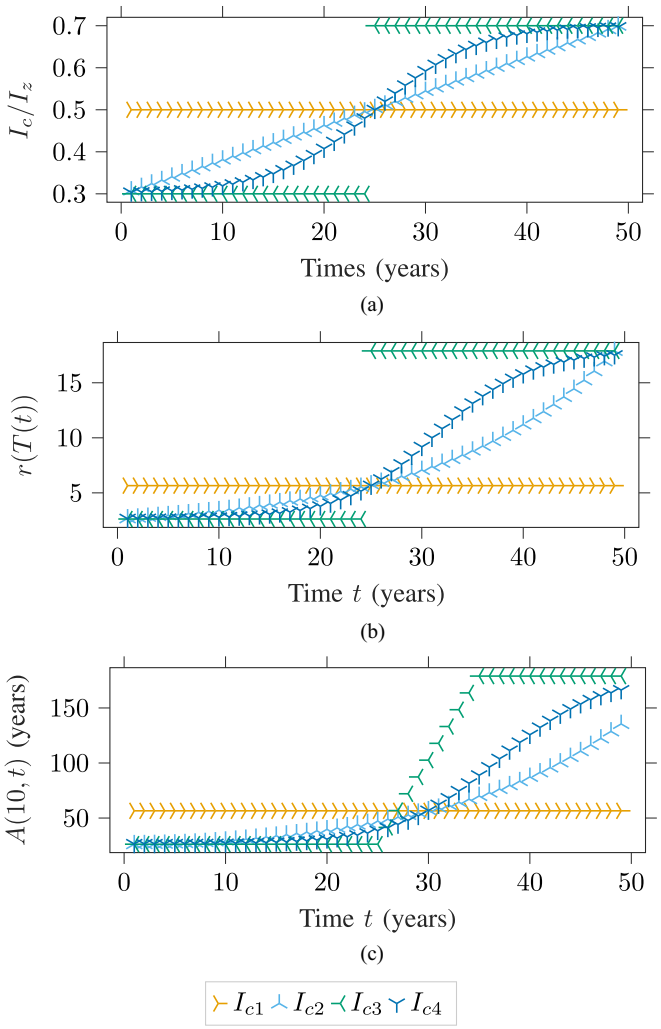


Fig. 6. Accelerated ageing under time-varying conductor currents. (a) Normalised current profiles I_c/I_z. (b) Ageing acceleration factor $r(T(t))$. (c) Effective age $A(10,t)$ of a cable with service age $a = 10$ years.

effective age of 10 years cables is around 30% lower for the second half of the transition.

The second experiment applies the annual line loading distributions for the three scenarios (without DER, PV-dominated and Wind-dominated) from Fig. 2 to PILC cables. We compute the temperatures (3). Fig. 7(a) shows the distribution over temperatures $\rho_T(T)$. We then model the energy transition (20) with $c_1 = 0.2$ and $c_2 = 25$ where ρ_0 is the initial distribution without DER, and we consider two cases where ρ_1 is either Wind-dominated or PV-dominated. As exemplarily shaded in the PV-dominated scenario, the cable is only operated 1.4% of the time above the rated temperature ($\frac{\int_{T_{\max}}^{\infty} \rho_T(T)\,dT}{\int_{-\infty}^{\infty} \rho_T(T)\,dT} = 1.4\%$ and see Fig. 7(a)). Fig. 7(b) shows the contribution of the temperature time-shares to the effective ageing. The 'area under the curve' is the cumulative contribution of the times that the cable is operated above the ampacity, i.e. applying (15). In the PV-dominated case, the 1.4% share of operating above the rated temperature causes 46% of the ageing ($\frac{\int_{T_{\max}}^{\infty} r(T)\,\rho_T(T)\,dT}{\int_{-\infty}^{\infty} r(T)\,\rho_T(T)\,dT} = 46\%$ and see

Authorized licensed use limited to: TU Delft Library. Downloaded on October 08,2026 at 07:45:28 UTC from IEEE Xplore. Restrictions apply.

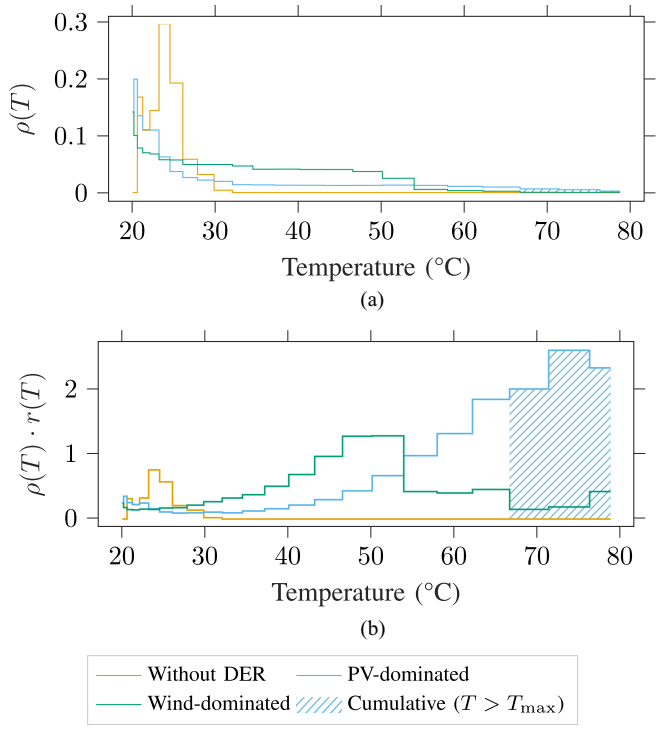


Fig. 7. Temperature distributions and their contribution to effective ageing for the loading scenarios in Fig. 2. (a) Temperature distributions $\rho(T)$. (b) Contribution to effective ageing $\rho(T) \cdot r(T)$, including the cumulative contribution for $T > T_{\max}$.

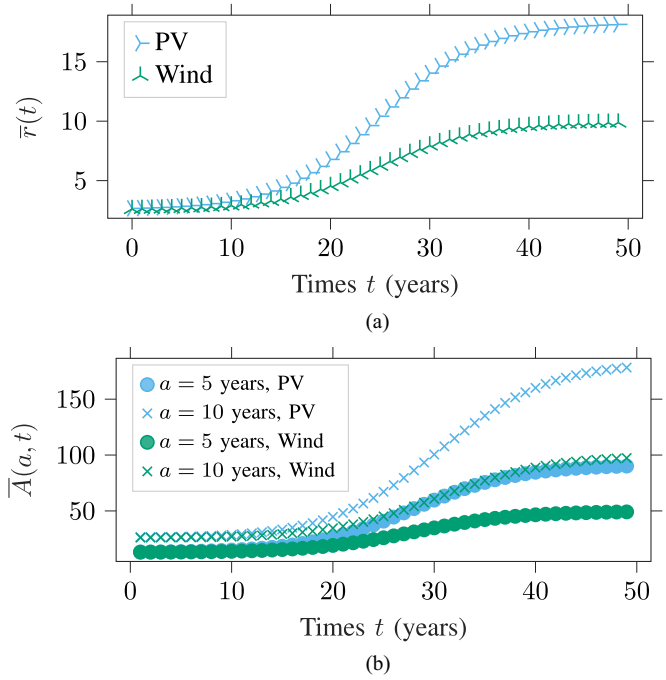


Fig. 8. (a) Time-varying ageing acceleration factor $\overline{r}(t)$ for PV- and wind-dominated scenarios. (b) Effective age $\overline{A}(a,t)$ of cables with service ages $a = 5$ years and $a = 10$ years under the same scenarios.

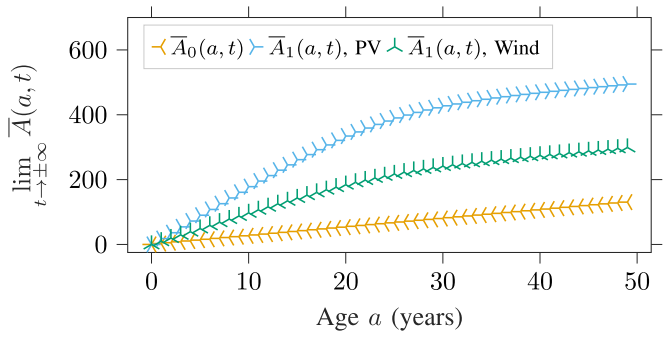


Fig. 9. The effective age for different cable ages a before ($\overline{A}_0(a)$) and after ($\overline{A}_1(a)$) the energy transition.

Fig. 7(b)). These results demonstrate that reliability behaviour under non-stationary stress can exhibit nonlinear amplification effects, where relatively small time shares at elevated loading levels disproportionately contribute to long-term degradation. Such behaviour cannot be captured by classical stationary Weibull models that assume constant stress exposure over time. Fig. 8(a) shows the effective ageing acceleration factor $\overline{r}(t)$ over time computed with (11). The PV-Dominated scenario leads to faster ageing than in the Wind-Dominated Scenario due to higher peak load, and more frequently exceeding the ampacity I_z (see Fig. 2). Fig. 6(c) shows the effective age $\overline{A}(a,t)$ of cables that are $a = 5$ and $a = 10$ years old, computed by (12) for PV and Wind dominated grids, respectively. Although a cable is just 10 years in service, the effective age surpasses 50 years already at the intermediate of the transition ($t = 25$ years) in the PV-scenario. This shows the fast acceleration of ageing in cables exposed to the energy transition. Fig. 9 shows the effective age $\overline{A}(a,t)$ for cables with actual age a at the limits ((24)), before and after the energy transition, $A_0(a)$ and $A_1(a)$, respectively. This shows the effective age is around $2-3$ times higher after the energy transition than before. One can also notice the high increase of effective ageing before 30 years.

D. Failure Statistics of an Aged Population of MV Cables

Two studies investigate the failure statistics of a population that has heterogeneous ages and where the age distribution changes with time. The first case study investigates the Weibull failure rate (9) under various operating conditions for an aged population of cables. Fig. 10 shows the failure rates for PILC and XLPE cables of varying ages when applying three different conductor currents I_c. These currents are steadily (constantly) applied to the cable, assuming $\alpha = 0$. These currents lead to different characteristic lives $\hat{\eta}$ using (4) and (5) and $\hat{\eta}_r$. This figure confirms that the failure rates drastically increase when permanently operated above the ampacity. The second case study simulates successively replacing PILC with XLPE cables when PILC cables fail, which represents a scenario that the Danish DSOs (and others) currently apply. Fig. 11 shows the age distributions of PILC and XLPE at the start of the simulation $t = 0$ years. The time t and ages a are considered discrete $\mathbb{N}$ with the unit 'years'. Fig. 12 shows the expected failures per year for a conductor current I_c permanently applied to these cables at $t = 0$ years. The applied current I_c leads to the operating temperature T, the characteristic lifetime $\hat{\eta}(T)$

Authorized licensed use limited to: TU Delft Library. Downloaded on October 08,2026 at 07:45:28 UTC from IEEE Xplore. Restrictions apply.

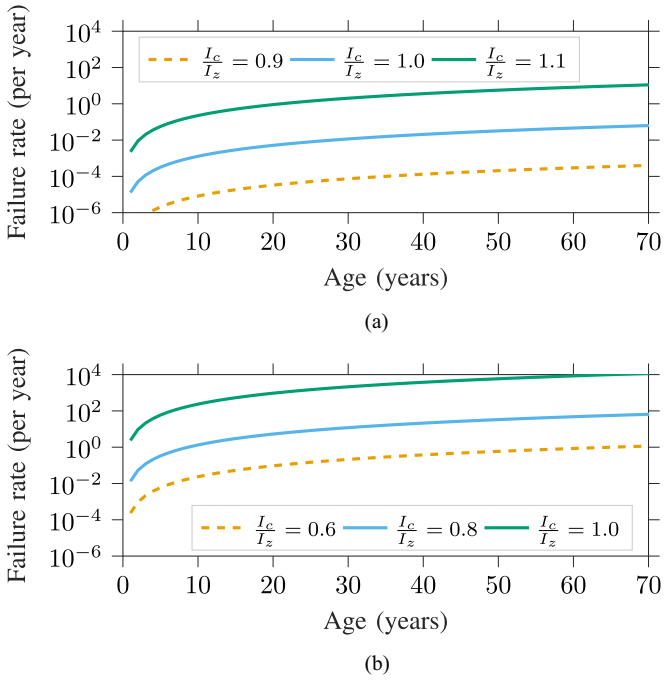


Fig. 10. Failure rate as a function of cable age for constant loading conditions. (a) XLPE cables for different conductor currents $\frac{I_c}{I_z}$. (b) PILC cables for different conductor currents $\frac{I_c}{I_z}$.

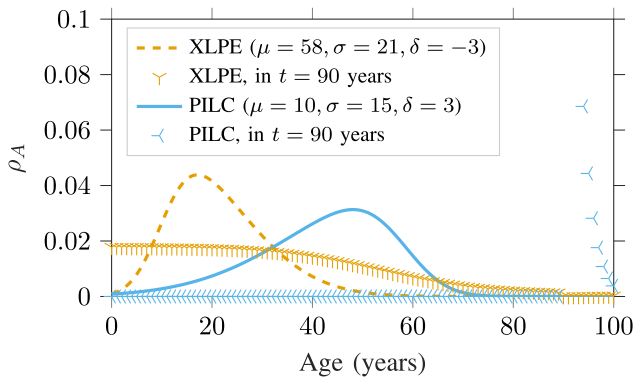


Fig. 11. The age distributions of XLPE and PILC.

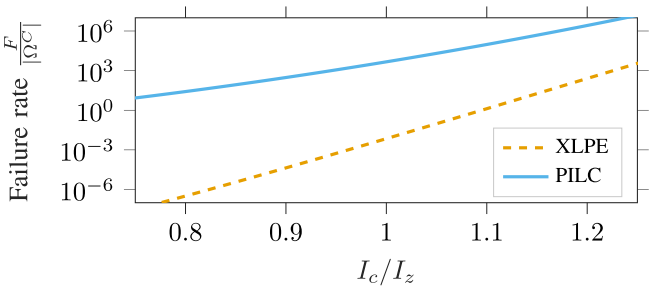


Fig. 12. Failures increase with I_c applied to XLPE and PILC cables.

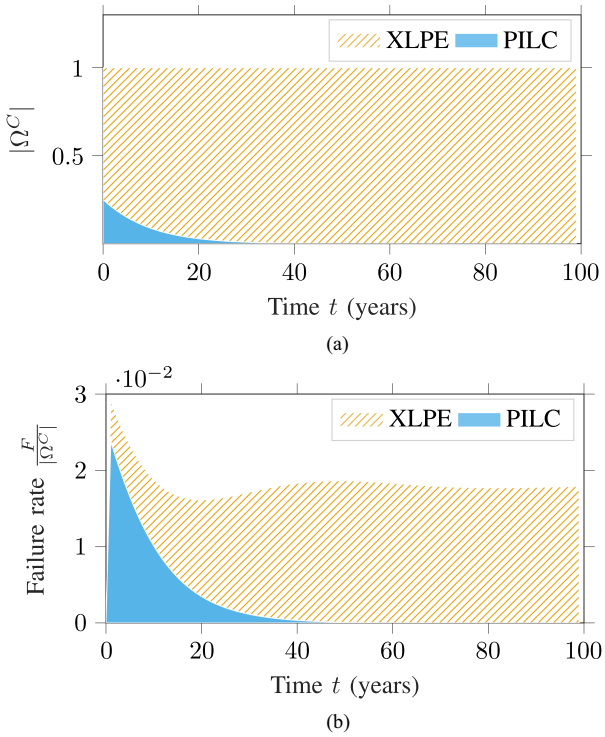


Fig. 13. Evolution of cable populations under *Run-to-failure* replacement. (a) Share of XLPE and PILC cables in the network over time. (b) Normalised failure-rate contribution $\frac{F}{|\Omega^C|}$ over time for XLPE and PILC cables.

and the Arrhenius-Weibull failure rate (9) used in (2). This figure shows the exponential increase in failure rates for the two cable types. Next, this study investigates the failures of a set of cables of varying ages, and when their age distribution changes with time, applying the *Run-to-failure* maintenance. All XLPE cables are assumed to operate at the constant $I_c = I_z$, and all PILC cables operate at the constant $I_c = 0.5I_z$. With time, all failed PILC cables are replaced with XLPE cables, and all failed XLPE cables are replaced in the following year by new XLPE cables. The replacement changes their age distributions. For example, the PILC distribution change is computed by $\rho_A(0,t) = 0$ and $\rho_A(a+1,t) = \rho_A(a,t-1)(1-\lambda(a))$ for $t = 1, \ldots 100$. Fig. 11 shows the distributions after $t = 90$ years, where the XLPE distribution reached some sort of steady-state and only a few very old PILC cables remained. Fig. 13(a) shows the change in the shares of these two cable types. After 20 years, nearly all PILC cables were replaced by XLPE, due to the high failure rate of PILC cables (Fig. 10) and their high age (Fig. 11). Fig. 13(b) shows the normalised failure rate $\frac{F}{|\Omega^C|}$. Despite only 25% of cables being of type PILC at $t = 0$, these cables cause around 82% of total failures in the system.

E. Assessing Maintenance Strategies

Two case studies investigate the shortcut method to assess maintenance strategies during the energy transition: the first study focuses on the energy scenarios from (7), and the second study considers spatial loading variability, focusing on the

Authorized licensed use limited to: TU Delft Library. Downloaded on October 08,2026 at 07:45:28 UTC from IEEE Xplore. Restrictions apply.

TABLE II
COMPARING MAINTENANCE INCREASE $\frac{N(t_1)}{N(t_0)}$ (–) OF THREE STRATEGIES APPLIED TO PILC AND XLPE IN PV AND WIND-DOMINATED SCENARIOS.

	PILC		XLPE	
	PV	Wind	PV	Wind
Run-to-failure	307	54	1,491,111	79,504
Replace-all	307	54	10.4	1.07
Preventive	254	44	1	1

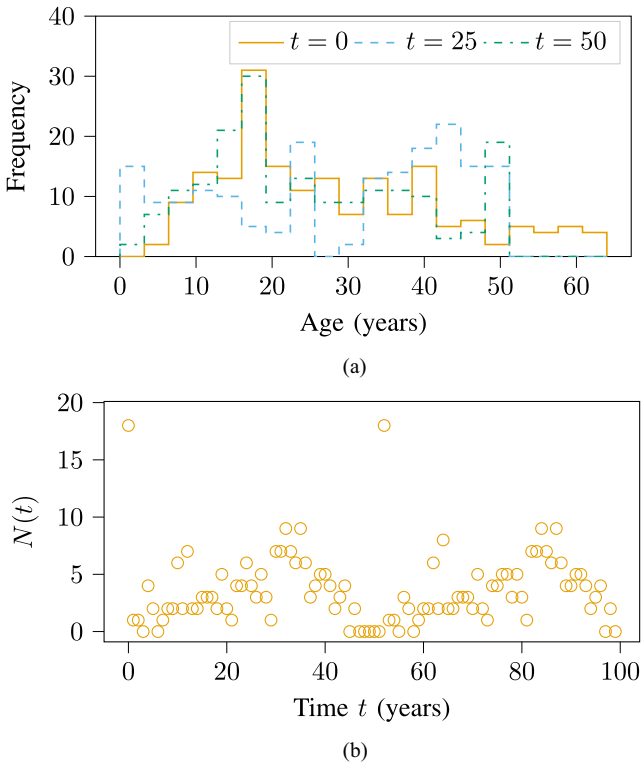


Fig. 14. *Replace-all* strategy applied to the Oberrhein system. (a) Histogram of the cable age distribution at $t = 0$, $t = 25$, and $t = 50$ years. (b) Annual number of replacements $N(t)$.

MV Oberrhein system. The first study assumes steady-state $\rho_A(a,t) = \rho_A(a)$ age distribution (from $t = 0$, Fig. 11). We use the load distributions from Fig. 7 for PV, and Wind-dominated at t_1 and Without DER at t_0, to assess the relative maintenance increase $\frac{N(t_1)}{N(t_0)}$ from before to after the energy transition. Table II shows the maintenance increase when applying the three strategies (applying equations (36), (40), and (45), respectively). For PILC cables, we observe around $250 - 300$ times increase in maintenance in the PV-Dominated and around times $45 - 55$ increase in the Wind-Dominated scenarios. The higher increase in the PV-dominated scenario over the Wind-Dominated scenario is due to more frequently operating the assets beyond and near the ampacities. For XLPE cables, the *Run-to-failure* maintenance strategy shows up to a million increases in maintenance as a very low $\overline{r}_0$ appears in (36) in the denominator as base with the exponent $\beta = 3.4$. Fig. 12 shows that the $\frac{I_c}{I_z}$ needs to be in ranges near 0.9 to lead to high failure rates in XLPE. However, Fig. 2 shows that before the transition at t_0 (Without DER) $\frac{I_c}{I_z} < 0.5$ meaning $\overline{r}_0$ is extremely low. In other words, a $\Delta\frac{I_c}{I_z} = 0.1$ increase can lead to a few magnitudes increase in failure rates

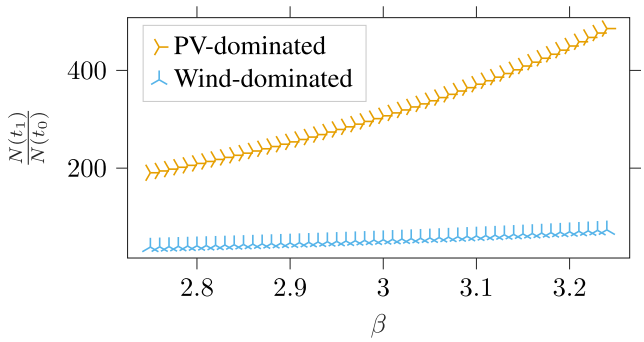


Fig. 15. Sensitivity of PILC results to the selection of β in *Run-to-failure*.

(see Fig. 12) and $\overline{r}$, where the increase in $\overline{r}$ in (36) has a power with the exponent $\beta = 3.4$. Further in Table II, the *Preventive* maintenance strategy does not lead to an increase in maintenance of XLPE cables, and the *Replace-all* strategy has a 10-fold increase for the PV-Dominated scenario.

The second study on the MV Oberrhein system investigates the *Replace-all* strategy. Each cable c of age a_c in year t is modelled as $Y \sim \text{Bernoulli}(\lambda(a_c,t))$, where $Y = 1$ indicates failure (with probability $\lambda(a_c,t)$) and $Y = 0$ survival (with probability $1 - \lambda(a_c,t)$). If a cable fails or $a_c > a_R$, the cable is replaced by the same type (PILC or XLPE) with age $a_c = 0$ in the following year. Fig. 14(a) shows the histogram of age distribution (aggregated for PILC and XLPE) at three times $t = \{0, 25, 50\}$ years. The distribution at $t = 0$ years and $t = 50$ years shows a high similarity. The age replacement $a_R = 50$ years leads to some periodicity in time with period 50 years. This also shows that scheduled replacement dominates over replacement due to failures. Fig. 14(b) shows the maintenance over time when applying (48), where the same periodicity appears. The peak of replacements per year reaches about 19 as these are at the start of the simulation, where a large fraction of PILC cables are replaced due to their age beyond 50 years (see Fig. 11). However, these simulations show averages of around 5 replacements per year, which seems high for 181 cables, demonstrating the inefficiency of the *Replace-all* strategy that does not consider asset health condition h_c.

F. Discussion on the Sensitivity of Results to Ageing Parameters

The results and conclusions of this work are highly sensitive to the ageing parameters. For example, when repeating the study in Section IV-E with varying values for β, Fig. 15 shows the sensitivity of the XLPE results in the *Run-to-failure* maintenance strategy. By varying β just a small fraction, one can see that the maintenance increase can change by a factor 2. This study shows high sensitivity on the shape parameter β that appears in the exponent to evaluate maintenance increase (36). Selecting the value β is important as it tremendously impacts the results, i.e., some references estimate β for all age-related modes of failures, not isolating only thermal ageing of cables. This sensitivity is also structurally supported by the analytical shortcut formulations, where β appears as an exponent in maintenance scaling

Authorized licensed use limited to: TU Delft Library. Downloaded on October 08,2026 at 07:45:28 UTC from IEEE Xplore. Restrictions apply.

relations (e.g. (36)), implying that small parameter variations propagate nonlinearly into maintenance predictions. At the same time, the literature shows a high variability in reported β. For example, data from [38] suggest values closer to $\beta = 6.3$, based on an average of four manufacturers. Overall, to fit an accurate β, we recommend conducting ageing (stress-tests) experiments to estimate failure rates under changes in operating conditions in an existing fleet of medium-voltage cables with heterogeneous ages. While β represents a dominant statistical uncertainty, other model parameters also influence the robustness of the quantitative predictions. Beyond the Weibull shape parameter β, the robustness of the quantitative results is mainly governed by parameters that influence the ageing acceleration factor $r(T)$, such as thermal ageing constants, temperature limits, and ampacity assumptions through the temperature model. Small variations in these parameters can lead to disproportionate changes in predicted maintenance because the shortcut formulations amplify changes in r, for example, through the relation $\frac{N(t_1)}{N(t_0)} = (\frac{r_1}{r_0})^{\beta}$ in the *Run-to-failure* strategy. This implies that uncertainties affecting operation close to ampacity have the strongest impact on results, while uncertainties affecting lower loading regimes have comparatively smaller influence. Overall, the results indicate that while quantitative maintenance estimates are sensitive to ageing and loading parameters, the qualitative findings regarding the dominant influence of high-loading periods and transition-driven ageing trends remain robust across plausible parameter variations. Consequently, the proposed framework is primarily intended to provide structurally reliable system-level insight, while absolute maintenance levels should be interpreted with consideration of parameter uncertainty. The present model assumes monotonic cumulative ageing and does not explicitly capture potential thermal recovery effects during extended low-loading periods. Incorporating recovery dynamics would require physics-based degradation modelling or state-dependent ageing formulations and represents a relevant direction for future research.

V. Conclusion

Time-varying loading of MV cables impacts the estimations of failure rates, estimated lifespan, and maintenance required. Considering time variation and loading variability is essential for reliability assessment in electricity systems undergoing the energy transition. The proposed approach combines probability estimates of the loading with shortcut methods to estimate maintenance increase before and after a systematic load change, such as during the energy transition. This method supports estimating on MV grid data from Denmark and Germany, where our case study demonstrates that the top 1.4% of times with the highest loading slightly above the ampacity causes 46% of thermal-related cable ageing. These changes specifically impact PILC cables, and operators may expect increasing failure rates. Our studies show up to $10 - 300$ times higher maintenance needs in the future, meaning that society may face a large financial burden of incorrectly performed maintenance. Overall, the results quantify how systematic increases in loading variability can significantly accelerate population-level ageing and maintenance demand. Qualitatively, the study reveals that reliability degradation under evolving operating conditions is dominated by nonlinear stress accumulation effects that are not captured by stationary reliability modelling assumptions. These findings also suggest operators need to carefully assess their maintenance strategies, failure models, and accurately estimate model parameters to guide society to a cost-efficient energy transition.

Acknowledgment

Some parts of the manuscript benefited from grammar and clarity improvements using automated tools, including Grammarly and ChatGPT. The authors remain responsible for all content.

Appendix

A. Temperature-Dependent Electrical Resistivity

The conductor temperature T can be estimated with (3) that can be expanded considering the material-specific temperature coefficient α as follows

$$T(\tau) = T_a + (T_{max} - T_a) \cdot \left(\frac{|I_c(\tau)|}{I_z} \right)^2 \cdot \frac{1 + \alpha \cdot (T(\tau - 1) - T_a)}{1 + \alpha \cdot (T_{max} - T_a)} \tag{49}$$

where $T(\tau - 1)$ refers to the previous time step. For steady conditions, one can consider $T(\tau) = T(\tau - 1)$, and either analytically solve this equation for T, or numerically approximate it, for example, using as initial point for $T(\tau - 1)$ from (3).

References

[1] R. Billinton and R. N. Allan, *Reliability Evaluation of Engineering Systems*, vol. 792. New York, NY, USA: Springer, 1992.
[2] M. Zapf et al., "Lifetime assessment of PILC cables with regard to thermal aging based on a medium voltage distribution network benchmark and representative load scenarios in the course of the expansion of distributed energy resources," *Energies*, vol. 14, no. 2, 2021, Art. no. 494.
[3] I. Grossoni et al., "Observed failures at railway turnouts: Failure analysis, possible causes and links to current and future research," *Eng. Failure Anal.*, vol. 119, 2021, Art. no. 104987.
[4] A. Gupta, P. Kumar, and R. Rastogi, "Critical review of flexible pavement performance models," *KSCE J. Civil Eng.*, vol. 18, no. 1, pp. 142–148, 2014.
[5] J. Z. Hansen, "Use of fault statistics for the management of aging medium voltage PILC cable systems," in *Proc. 25th Int. Conf. Exhib. Electricity Distrib.*, Madrid, Spain: Association des Ingénieurs de Montefiore, 2019, Paper no. 1123. [Online]. Available: http://dx.doi.org/10.34890/532
[6] J. Z. Hansen, "Results from danish failure statistics for medium voltage XLPE cables," in *Proc. 22nd Int. Conf. Exhib. Electricity Distrib.*, 2013, pp. 1–4.
[7] K. Sundsgaard, "Predictive maintenance of medium voltage cable networks using machine learning: A data-centric approach for the electricity distribution industry in denmark," Ph.D. dissertation, Tech. Univ. Denmark, Kongens Lyngby, Denmark, 2025.
[8] J. Z. Hansen, "Failure statistic for medium voltage cable systems in Denmark," in *Proc. 27th Int. Conf. Electricity Distrib.*, 2023, vol. 2023, pp. 2208–2212.
[9] G. P. Denmark, "Fejl- og afbrudsstatistik 2013-2022," Green Power Denmark, Copenhagen, Denmark, Tech. Rep. RA646, 2023.
[10] A. Rafati et al., "Power grid renovation: A comprehensive review of technical challenges and innovations for medium voltage cable replacement," *Smart Cities*, vol. 7, no. 6, pp. 3727–3763, 2024.

Authorized licensed use limited to: TU Delft Library. Downloaded on October 08,2026 at 07:45:28 UTC from IEEE Xplore. Restrictions apply.

[11] J. Heres, R. Stijl, and F. Reinders, "Machine learning methods for the health-indexing and ranking of underground distribution cables and joints," in *Proc. CIRED Workshop*, pp. 1–4, doi: 10.1049/cp.2016.0751.
[12] M. H. P. Klerx, J. Morren, and H. Slootweg, "Analyzing parameters that affect the reliability of low-voltage cable grids and their applicability in asset management," *IEEE Trans. Power Del.*, vol. 34, no. 4, pp. 1432–1441, Aug. 2019.
[13] M. Bindi, A. Luchetta, G. M. Lozito, C. F. M. Carobbi, F. Grasso, and M. C. Piccirilli, "Frequency characterization of medium voltage cables for fault prevention through multi-valued neural networks and power line communication technologies," *IEEE Trans. Power Del.*, vol. 38, no. 5, pp. 3227–3237, Oct. 2023.
[14] M. Bindi et al., "A comprehensive review of fault diagnosis and prognosis techniques in high voltage and medium voltage electrical power lines," *Energies*, vol. 16, no. 21, 2023, Art. no. 7317.
[15] M. Abdolahi, W. Song, and M. Yazdani-Asrami, "Intelligent condition monitoring of power cables using advanced machine learning models," *Results Eng.*, vol. 29, 2026, Art. no. 108371.
[16] F. Steennis et al., "Smart cable guard for pd-online monitoring of MV underground power cables in Stedin's network," in *Proc. Int. Conf. Condition Monit. Diagnosis*, vol. 2014, 2014, pp. 525–528.
[17] S. Rieken et al., "A scalable approach towards real-time cable ratings for underground medium voltage cables," in *Proc. CIRED 26th Int. Conf. Exhib. Electricity Distrib.*, 2021, vol. 2021, pp. 109–113.
[18] A. S. Alghamdi and R. K. Desuqi, "A study of expected lifetime of XLPE insulation cables working at elevated temperatures by applying accelerated thermal ageing," *Heliyon*, vol. 6, no. 1, 2020, Art. no. e03120.
[19] S. Qin et al., "Study on temperature rise characteristics of 110 kV XLPE cable under different service years considering dielectric loss," *Energy Rep.*, vol. 8, pp. 493–501, 2022.
[20] C. Weindl et al., "Development of the P-factor in an accelerated ageing experiment of the MV PILC cables," in *Proc. 10th IEEE Int. Conf. Solid Dielectrics*, 2010, pp. 1–4.
[21] I. Mladenovic and C. Weindl, "Artificial aging and diagnostic measurements on medium-voltage, paper-insulated, lead-covered cables," *IEEE Elect. Insul. Mag.*, vol. 28, no. 1, pp. 20–26, Jan./Feb. 2012.
[22] V. Montsinger, "Loading transformers by temperature," *Trans. Amer. Inst. Elect. Engineers*, vol. 49, no. 2, pp. 776–790, 1930.
[23] L.-J. Wei, "The accelerated failure time model: A useful alternative to the cox regression model in survival analysis," *Statist. Med.*, vol. 11, no. 14/15, pp. 1871–1879, 1992.
[24] M. H. S. Siddiqui et al., "Dynamic state transition model-based prognosis approach for degradation prediction of aerial bundled cables," *Res. Square*, 2025, preprint, Version 1, 11 Jun. 2025. [Online]. Available: https://doi.org/10.21203/rs.3.rs-6738017/v1
[25] Energy Networks Association, "DNO common network asset indices methodology (version 2.1)," Apr. 2021. Accessed: Aug. 15, 2025. approved by Ofgem. [Online]. Available: https://www.ofgem.gov.uk/sites/default/files/docs/2021/04/dno_common_network_asset_indices_methodology_v2.1_final_01-04-2021.pdf
[26] L. Chmura et al., "Review of the residual life assessment of high-voltage cables by means of bottom-up and top-down analysis - Dutch experience," *Gaodianya Jishu*, vol. 41, no. 4, pp. 1114–1124, 2015.
[27] S. Bottler, T. Blenk, and C. Weindl, "An approach for determining load-dependent monetary assessment factors for PILC and XLPE cables within a load flow simulation," in *Proc. Glob. Energy Conf.*, 2022, pp. 58–64.
[28] M. A. Miner, "Cumulative damage in fatigue," *J. Appl. Mechan.*, vol. 12, no. 3, pp. A159–A164, 1945.
[29] J. L. Klimenta et al., "Thermal aging management for electricity distribution networks: FEM-based qualification of underground power cables," *Thermal Sci.*, vol. 26, no. 4, pp. 3571–3586, 2022.
[30] W. Higinbotham and K. Higinbotham, "Review of medium voltage asset failure investigations," *Prem. Electr. Maint. Saf. Event*, vol. 1, 2018, Art. no. 17.
[31] L. Bertling, R. Allan, and R. Eriksson, "A reliability-centered asset maintenance method for assessing the impact of maintenance in power distribution systems," *IEEE Trans. Power Syst.*, vol. 20, no. 1, pp. 75–82, Feb. 2005.
[32] C. Zhou, H. Yi, and X. Dong, "Review of recent research towards power cable life cycle management," *High Voltage*, vol. 2, no. 3, pp. 179–187, 2017.
[33] S. Sachan et al., "Stochastic dynamic programming approach for proactive replacement of power cables," in *Proc. CIRED Workshop*, 2016, pp. 1–4, doi: 10.1049/cp.2016.0680.
[34] O. L. Hestad, F. Mauseth, and R. H. Kyte, "Electrical conductivity of medium voltage XLPE insulated cables," in *Proc. IEEE Int. Symp. Elect. Insul.*, 2012, pp. 376–380.
[35] *Power Cables With Extruded Insulation and Their Accessories for Rated Voltages From 1 kV (Um = 1,2 kV) up to 30 kV (Um = 36 kV) - Part 2: Cables for Rated Voltages From 6 kV (Um = 7,2 kV) up to 30 kV (Um = 36 kV)*, IEC Standard 60502-2:2014, International Electrotechnical Commission, Geneva, Switzerland, 2014.
[36] *Electric Cables - Calculation of the Current Rating - Part 1-1: Current Rating Equations (100 % Load Factor) and Calculation of Losses - General*, IEC Standard 60287-1-1:2006+AMD1:2014 CSV, International Electrotechnical Commission, Geneva, Switzerland, 2014.
[37] *Specification for Impregnated Paper-Insulated Lead or Lead-Alloy Sheathed Electric Cables of Rated Voltages up to and Including 33 000 v*, BS Standard 6480, British Standards Institution, London, U.K., 1988.
[38] Y. Tang et al., "Reliability evaluation of 10kV xlpe cable based on fault correlation Bayesian network and weibull distribution model," in *Proc. IEEE 4th Int. Conf. Elect. Mater. Power Equip.*, 2023, pp. 1–4.

Authorized licensed use limited to: TU Delft Library. Downloaded on October 08,2026 at 07:45:28 UTC from IEEE Xplore. Restrictions apply.